

Available online at www.sciencedirect.com

ScienceDirect

journal homepage: www.jfda-online.com

Original Article

Curculigoside and polyphenol-rich ethyl acetate fraction of *Molineria latifolia* rhizome improved glucose uptake via potential mTOR/AKT activated GLUT4 translocation



Der Jiun Ooi ^a, Nur Hanisah Azmi ^a, Mustapha Umar Imam ^{a,1},
Noorjahan Banu Alitheen ^b, Maznah Ismail ^{a,*}

^a Nutri-Cosmeceuticals, Nutrigenomics & Nanodelivery Programme, Laboratory of Molecular Biomedicine, Institute of Bioscience, Universiti Putra Malaysia, 43400, Serdang, Selangor, Malaysia

^b Department of Cell and Molecular Biology, Faculty of Biotechnology and Biomolecular Sciences, Universiti Putra Malaysia, 43400, Serdang, Selangor, Malaysia

ARTICLE INFO

Article history:

Received 13 October 2017

Received in revised form

14 February 2018

Accepted 13 March 2018

Available online 5 April 2018

Keywords:

Curculigoside

Ethyl acetate fraction

Glucose uptake

GLUT4 translocation

mTOR/AKT activation

ABSTRACT

Adipose tissue is one of the major organs responsible for rapid restoration of postprandial glucose fluxes. Being the major isoform of glucose transporter in adipose tissue, regulations of insulin-dependent GLUT4 trafficking have always been of research interest. The present study aimed to examine the molecular mechanisms underlying the efficacy of curculigoside and polyphenol-rich ethyl acetate fraction (EAF) of *Molineria latifolia* rhizome in triggering glucose uptake. We assessed the adipogenic potential and glucose uptake stimulatory activity of curculigoside and EAF by employing a murine 3T3-L1 adipocyte model. The transcriptional and translational expressions of selected intermediates in the insulin signalling pathway were evaluated. While curculigoside neither promoted adipogenesis nor activated peroxisome proliferator activated receptor gamma, treatment with polyphenol-rich EAF resulted otherwise. However, both treatments enhanced insulin-stimulated uptake of glucose. This was coupled with increased availability of GLUT4 at the plasma membrane of the differentiated adipocytes although the total GLUT4 protein level was unaffected. In addition, the treatment increased the phosphorylation of both AKT and mTOR, which have been reported to be associated with GLUT4 translocation. The present findings proposed that curculigoside and EAF increased glucose transport activity of 3T3-L1 adipocytes via GLUT4 translocation as a result of potential mTOR/AKT activation. The more potent efficacy observed with EAF suggested potential synergistic and multi-targeted action.

Copyright © 2018, Food and Drug Administration, Taiwan. Published by Elsevier Taiwan LLC. This is an open access article under the CC BY-NC-ND license (<http://creativecommons.org/licenses/by-nc-nd/4.0/>).

Abbreviations: EAF, ethyl acetate fraction.

* Corresponding author. Fax: +603 8947 2116.

E-mail addresses: myhome.e@gmail.com, maznahis@upm.edu.my (M. Ismail).

¹ Present address. Department of Medical Biochemistry, Usmanu Danfodiyo University, P.M.B. 2346, Sokoto, Nigeria.

<https://doi.org/10.1016/j.jfda.2018.03.003>

1021-9498/Copyright © 2018, Food and Drug Administration, Taiwan. Published by Elsevier Taiwan LLC. This is an open access article under the CC BY-NC-ND license (<http://creativecommons.org/licenses/by-nc-nd/4.0/>).

1. Introduction

Solute carrier family 2, facilitated glucose transporter member 4 (SLC2A4) or commonly known as GLUT4, is a member of the sugar transporter proteins which catalyses the ATP-independent trans-membrane transport of hexose sugar. It is also the major isoform of glucose transporter expressed in adipose tissue. At the basal state, GLUT4 predominantly resides in the intracellular vesicular compartment. In the presence of insulin, the exocytic rate of GLUT4 vesicle increases, leading to translocation of the protein to the plasma membrane [1]. An increased availability of the transporter protein on the cell surface thus enhances uptake of glucose.

Insulin resistance is a condition whereby normal insulin level is ineffective in triggering desired response in glucose disposal organs such as adipose and skeletal muscle tissues. Diminished glucose uptake by these cells leads to impaired glucose homeostasis, elevated blood glucose level and ultimately, diabetes mellitus [2]. The use of insulin sensitising agents such as thiazolidinediones to antagonise insulin resistance has thus become one of the treatment options for type 2 diabetes. Thiazolidinediones function as agonists for peroxisome proliferator activated receptor gamma (PPAR γ) and promote adipocyte differentiation [3]. Despite their potent anti-hyperglycaemic action, thiazolidinediones have restricted usage in the clinical management of diabetes owing to the occurrence of several side effects, including weight gain, bone fracture, congestive heart failure and potential bladder cancer [4,5].

Therefore, identification of novel bioactive compounds as a safer alternative to increase insulin sensitivity has always been of research interest. Curculigoside, a type of phenolic glycoside, has been reported to exhibit anti-oxidative, neuro-protective and anti-osteoporotic capabilities [6–9]. The compound, previously isolated from the rhizome of *Curculigo orchoides* Gaertn. [10], is also identified in *Molineria latifolia* (Dryand. ex W.T.Aiton) Herb. ex Kurz [11]. Both plants are highly related species and belong to the Hypoxidaceae family. The extract of *M. latifolia* had been reported to exhibit anti-diabetic and hypolipidemic activities *in vivo* [12], potentially due to the presence of curculigoside.

Owing to particular interest in the use of polyphenols as pharmaceutical alternatives, the development and formulation of polyphenol-rich ethyl acetate fraction (EAF) from *M. latifolia* constitutes effort to maximise the potential of polyphenols and to improve quality assurance [13]. In the present study, both polyphenol-rich EAF and curculigoside (one of the major compounds present in EAF) were evaluated for their cytotoxic effects and abilities to induce the process of adipogenesis in 3T3-L1 preadipocytes. Additionally, the efficacies of curculigoside and EAF in triggering glucose uptake in differentiated 3T3-L1 cells were also examined using 2-NBDG glucose analogue. Transcriptional and translational levels of selected intermediates participating in the insulin signalling pathway were also studied to understand the underlying molecular mechanism of action.

2. Materials and methods

2.1. Chemicals

3T3-L1 mouse fibroblast was obtained from American Type Culture Collection (Manassas, VA, USA). Curculigoside was purchased from Biopurify Phytochemicals (Sichuan, China). Dulbecco's modified eagle medium (DMEM), methylthiazolyldiphenyl-tetrazolium bromide (MTT), protease and phosphatase inhibitor cocktails, NP-40, BCA protein assay kit and Chemi-Lumi One L were purchased from Nacalai Tesque (Kyoto, Japan). Cinnamic acid, foetal bovine serum, bovine calf serum, gentamicin, dexamethasone, 3-isobutyl-1-methylxanthine, rosiglitazone, bovine serum albumin, bovine insulin and oil-red-o were purchased from Sigma (St. Louis, MO, USA). 2-NBDG (2-(N-(7-Nitrobenz-2-oxa-1,3-diazol-4-yl)Amino)-2-Deoxyglucose) and trizol reagent were purchased from Life Technologies Ltd. (Paisley, UK). GenomeLab™ GeXP Start Kit was purchased from Beckman Coulter Inc. (Miami, FL, USA), while 0.45 μ m Immobilon-FL polyvinylidene fluoride (PVDF) membrane and rabbit anti-GLUT4 primary antibody were purchased from Millipore (Bedford, MA, USA). Rabbit anti-insulin receptor beta, anti- α tubulin, anti-protein kinase B (PKB/AKT), anti-phospho AKT (Ser473), anti-mechanistic target of rapamycin (mTOR) and anti-phospho mTOR (Ser2448) primary antibodies and horseradish peroxidase-conjugated goat anti-rabbit secondary antibody were purchased from Cell Signaling Technology (Danvers, MA, USA). All the other chemicals were purchased from Sigma–Aldrich Co. (St. Louis, MO, USA).

2.2. Preparation of EAF

M. latifolia rhizomes were collected from Beranang, Selangor, Malaysia (Geographical Coordinates: 2.8833° N, 101.8667° E). A voucher specimen of the plant (SK 1709/09) was confirmed and deposited in the Biodiversity Unit, Institute of Bioscience, Universiti Putra Malaysia, Serdang, Selangor, Malaysia. The plant name was cross-checked for accuracy according to The Plant List [14]. Briefly, the collected rhizomes were oven dried at 40 °C, ground into fine particles and passed through a 30-mesh sieve. The *M. latifolia* rhizome powder was subsequently extracted thrice with 80% methanol. After filtration and removal of residual solvent, a 7.95% (w/w) yield for the crude extract was obtained. Part of the crude extract was dissolved in water, followed by a bio-guided fractionation using n-hexane, ethyl acetate and n-butanol respectively. Among the derived fractions, ethyl acetate fraction (EAF) showed the highest total phenolic content [11] and was therefore subjected to further analysis in the present study. The EAF was prepared in 0.1% (v/v) dimethyl sulfoxide (DMSO) and stored at –20 °C until use.

2.3. Cell culture

3T3-L1 mouse fibroblast cells were maintained in DMEM supplemented with 4.5 g/L D-glucose, 4 mM glutamine, 10%

bovine calf serum (v/v) and 50 µg/mL gentamicin in a humidified atmosphere of 5% CO₂ at 37 °C. Routine subculture was performed every 3–4 days until the cells were at approximately 80% confluence. Cells with passage number between 20 and 25 were used for experiments.

2.4. MTT cell viability assay

Cell viability was assessed by MTT colourimetric assay as reported by Foo et al. [15], with slight modifications. DMSO (0.1%; v/v) and Triton X-100 (1.0%; v/v) in DMEM were respectively being employed as vehicle control and positive control. The cell viability was expressed as fraction of viable cells relative to vehicle control cultures. The IC₂₀ and IC₅₀ values, indicating respective growth inhibitory doses, were calculated using Graphpad Prism 6.01 (San Diego, California, USA) with the 4 parameter logistic function standard curve analysis.

2.5. 3T3-L1 pre-adipocyte differentiation

Differentiation of 3T3-L1 cells was performed following the guideline provided by American Type Culture Collection (Manassas, VA, USA) (ATCC Tech bulletin #9). The cells were first seeded into 24-well culture plate at a density of 3×10^4 cells/well and further incubated until 100% confluence. The differentiation process (day 1) was initiated by incubating the cells in differentiation medium comprising of DMEM with 10% FBS (v/v), 50 µg/mL gentamicin, 1.0 µM dexamethasone, 0.5 mM IBMX and 1.0 µg/mL insulin. Fresh differentiation medium was supplied after every 48 h of incubation. On day 5, the differentiation medium was replaced with adipocyte maintenance medium consisting of DMEM with 10% FBS (v/v), 50 µg/mL gentamicin and 1.0 µg/mL insulin. The replacement of fresh medium after every 48 h incubation period proceeded until day 12. Test samples at non-toxic concentrations were included in the culture medium from day 1 for examining their ability to induce differentiation. Test samples at non-toxic concentrations were included in the culture medium from day 1 for examining their ability to induce differentiation. Control cultures were treated with either 20 µL of DMSO (0.1%; v/v) or rosiglitazone.

2.6. Cellular lipid determination

Cellular lipid content was determined by Oil Red O staining as reported by Beh et al. [16]. After the 12-day adipocyte differentiation, the differentiated cells were washed with PBS and further fixed with 4% neutral buffered formalin (v/v) for one hour at room temperature. After three times of PBS wash, the cells were then stained with 200 µL of Oil Red O (60%; v/v) solution for 30 min. Excess Oil Red O solution was subsequently aspirated. The stained cells were washed with PBS, allowed to air dry and photographed using Olympus DP80 Microscope Digital Camera (Tokyo, Japan). The lipid contents were quantified by measuring the spectrophotometric absorbance of the isopropanol-dissolved Oil Red O stain at 520 nm. The relative lipid content was calculated as:

$$\text{Relative lipid content (\%)} = \left(\frac{A_T}{A_C} \right) \times 100\%$$

where A_T is the absorbance of test wells and A_C is the absorbance of 0.1% DMSO (v/v)-treated control wells.

2.7. 2-NBDG uptake assay

Simulated glucose uptake activity was performed using fluorescently-labelled 2-NBDG glucose analogue based on the modified protocol described by Jung et al. [17]. Briefly, 3T3-L1 adipocytes differentiated on 96-well clear bottom black fluorescence plates (Thermo Scientific, Pittsburgh, PA, USA) were washed twice with PBS and incubated with 200 µL of starving medium (serum and glucose free DMEM) for 3 h. The medium was then removed. Subsequently, 200 µL of fresh starving medium supplemented with 100 µM 2NBDG, in the presence or absence of insulin (100 nM) and the different concentrations of test samples, were added and further incubated for 60 min. The cultures treated with either 20 µL of DMSO (0.1%; v/v) or rosiglitazone (5–20 µM) were employed as control reference. After the 60 min incubation, the cells were washed three times with ice-cold PBS to remove excess 2-NBDG and to stop the glucose uptake activity. The amount of retained fluorescence signal was determined fluorometrically at excitation wavelength of 485 nm and emission wavelength of 520 nm with a Biotek Synergy H1 Multi-Mode Reader (Winooski, VT, USA). The result was expressed as normalized fluorescence unit relative to control, indicating the ratio metric uptake of 2-NBDG.

2.8. GeXP multiplex gene expression analysis

Total RNA from the treated adipocytes was extracted using trizol reagent. Reverse transcription into cDNA and its amplification by PCR were conducted using the GenomeLab GeXP kit (Beckman Coulter, USA), according to the manufacturer's protocol in an XP Thermal Cycler (Bioer Technology, Germany). The PCR products were analysed on GeXP genetic analysis system, and the results were normalized using eXpress Profiler software following the manufacturer's instructions. Sequences of the primers are reported in [supplementary Table 1](#). Results were expressed as the ratio of the mRNA of interest to beta actin mRNA.

2.9. Subcellular fractionation and GLUT4 translocation analysis

Subcellular fractionation was performed based on the modified protocol described by Nishiumi and Ashida [18]. Following incubation, the cells were scraped in buffer A (pH 7.4), comprising of 50 mM Tris-HCl, 0.5 mM DTT, 0.1% NP-40 (v/v), protease and phosphatase inhibitors cocktails. After homogenisation, the mixture was mixed by passing through a 25-gauge needle for at least five times. The resulting lysate was then centrifuged at $1000 \times g$ for 10 min at 4 °C. The pellet was re-suspended in buffer A without NP-40, incubated for 10 min on ice and later centrifuged at $1000 \times g$ for 10 min at 4 °C. The pellet obtained after the second centrifugation was re-suspended in buffer A with 1% NP-40 (v/v) and further incubated for 1 h on ice. Following centrifugation at $14,000 \times g$ for 30 min at 4 °C, the supernatant containing plasma membrane was collected.

In order to obtain total cell lysate, the adherent cells were lysed with lysis buffer containing 50 mM Tris–HCl (pH 7.4), 150 mM NaCl, 1.0% NP-40 (v/v), 0.5% sodium deoxycholate (w/v), 0.1% SDS (w/v), 0.5 mM DTT, protease and phosphatase inhibitors cocktails. After centrifugation at $14,000 \times g$ for 30 min at 4 °C, the supernatant containing total cell lysate was collected. Quantification of protein in the plasma membrane and total cell lysate fraction was performed using BCA protein assay kit. The samples were stored in –80 °C until further use.

2.10. Immunoblotting

Equal amount of proteins (60 µg) were subjected to electrophoresis separation in 10% SDS-PAGE and semi-dry transferred to PVDF membrane. After blocking for 30 min with 5% BSA (w/v) in Tris-buffered saline containing Tween-20 (TBST), the membrane was probed with anti-GLUT4 (1:20 dilution), anti-insulin receptor beta (1:1000), anti-AKT (1:2000), anti-phospho AKT (1:1000), anti-mTOR (1: 2000), anti-phospho mTOR (1:1000) and anti-tubulin (1:3000) primary antibodies overnight at 4 °C. Following TBST wash, the membrane was further incubated with HRP-conjugated anti-rabbit IgG antibody (1:2000) for 1 h at room temperature. Immunoreactive bands were revealed using Chemi-Lumi One L. The image was captured using ChemiDoc MP System (Bio-Rad, Hercules, CA, USA) and the relative densities of the bands were analysed using Image Gauge Ver. 4.0 software (Fujifilm Life Science, Düsseldorf, Germany).

2.11. Statistical analysis

Results were expressed as mean \pm standard deviation. The statistical significance of differences was determined by ANOVA and Tukey's test using Graphpad Prism 6.01 (San Diego, California, USA). For all analyses, $p < 0.05$ was considered to be statistically significant.

3. Results and discussion

3.1. Cell viability assessment

The MTT assay was performed to determine the effects of curculigoside and EAF on the viability of 3T3-L1 preadipocytes following a 48 h challenge (Supplementary Fig. 1). The assay assesses the metabolic activity of viable cells by measuring the amount of insoluble formazan precipitate. Growth inhibitory doses, IC_{20} and IC_{50} values, were subsequently computed. The untreated vehicle control samples were assumed to be 100% viable while the positive controls led to 0% viability.

Based on the results, both curculigoside and EAF caused dose-dependent alterations on the viability of 3T3-L1 preadipocytes. The curculigoside had the respective IC_{20} and IC_{50} values of 88.59 ± 7.27 and 393.12 ± 47.51 µg/mL. On the other hand, the IC_{20} and IC_{50} values for EAF were 111.73 ± 9.57 and 509.59 ± 49.75 µg/mL, respectively. The 3T3-L1 preadipocytes treated with concentrations lower than 200 µg/mL were further observed under the phase contrast microscope. Although the treatment concentrations affected cell number,

no indication of cellular toxicity with regard to morphologic appearance changes was noted. Thus, concentrations of 50, 100 and 200 µg/mL of curculigoside and EAF were employed in the study.

3.2. Curculigoside and EAF have differing effects on adipogenesis

Although previously perceived to act passively on energy homeostasis, adipocytes have recently become important research targets for obesity and other metabolic diseases. During the process of adipogenesis, preadipocytes undergo cell differentiation process into mature adipocytes. Increase in number and size of the mature adipocytes lead to expansion of the white adipose tissue and subsequently, obesity [19,20]. Hence, control of adipocytes formation is a crucial strategy for anti-obesity therapy.

In the current study, 3T3-L1 cells were treated with various concentrations of curculigoside or EAF during the differentiation period to determine their effects on adipogenesis. After the 12-day differentiation period, the differentiated adipocytes were stained with Oil Red O, fixed and photographed (Fig. 1A). Quantification of the accumulated intracellular lipid contents (Fig. 1B) demonstrated that rosiglitazone, being the positive control, promoted adipogenesis in a dose-dependent manner. Increased intracellular lipid contents ranging from 1.2- to 1.7-fold ($p < 0.05$) were observed when compared to the control.

As treatments of both curculigoside and EAF affected the cell number of 3T3-L1 preadipocytes, the present results were normalized against the number of living cells in order to depict the actual findings. Briefly, treatment with 200 µg/mL of EAF increased the intracellular lipid content by 1.6-fold ($p < 0.01$). On the other hand, being one of the major bioactive present in EAF, curculigoside did not promote nor inhibit adipogenesis. These were depicted by the indifferent relative Oil Red O-stained contents in comparison to the control.

Intracellular and extracellular reactive oxygen species promote the process of adipogenic differentiation via PPAR γ activation. The use of mitochondrial-targeted antioxidant and restoration of the homeostatic redox balance may thus inhibit the differentiating process [21,22]. In the present study, curculigoside and EAF demonstrated dissimilar effects on adipogenesis although they were previously reported to exhibit potent antioxidant efficacy [8,11]. It is important to note that while anti-oxidative activity may play a role in affecting adipocyte differentiation, the formation of adipocytes from its precursors involves a complex network of transcriptional regulation [23,24]. More research explorations are thus needed. In order to provide some insights into the molecular mode of actions, the transcriptional expression of PPAR γ was further investigated in the present study.

3.3. Curculigoside and EAF increased 2-NBDG uptake in 3T3-L1 adipocytes

Adipocytes are one of the major insulin-responsive tissues responsible for maintaining the normal glucose homeostasis. In the presence of insulin, glucose is preferentially utilised for energy metabolism. Conversely, during low insulin levels, the

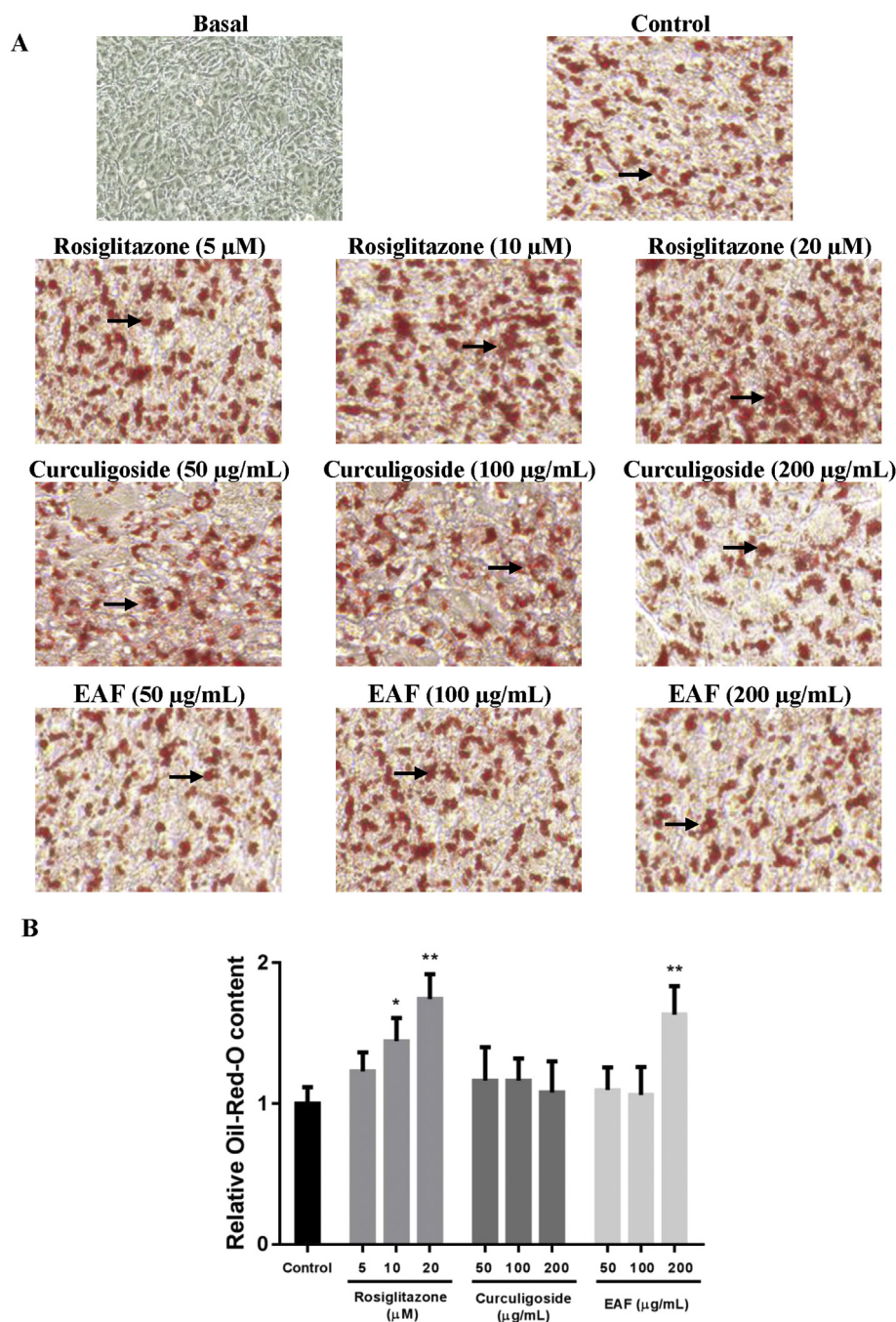


Fig. 1 – Effects of rosiglitazone, curculigoside and EAF on adipogenesis in 3T3-L1 cells. (a) Microscopic images of randomly selected 3T3-L1 adipocytes on day 12. Arrows indicate lipid droplets. Oil Red O-stained, 40 \times magnification. (b) Relative lipid content. The 0.1% DMSO (v/v)-treated culture served as control. Values are expressed as mean \pm standard deviation (n = 6). *p < 0.05 and **p < 0.01 compared to the control.

uptake of glucose reduces and shifts to ketone/free fatty acid metabolism [24]. The present study employed the use of fluorescently-labelled 2-NBDG glucose analog for the purpose of tracing glucose utilisation. The results were normalized against the number of living cells (Fig. 2).

Incubation of differentiated 3T3-L1 adipocytes with 200 μ g/mL of curculigoside and EAF enhanced the uptake of the non-metabolisable fluorescent 2-NBDG glucose analogue by respectively 1.6- and 1.9-fold (p < 0.01) at the basal state

without insulin. In the presence of insulin, both curculigoside and EAF further increased the uptake of glucose analogue. The insulin-stimulated enhancements of glucose analogue uptake in the presence of both curculigoside and EAF were dose-dependent. In the case of curculigoside, the lowest concentration did not trigger any significant responses. Nevertheless, medium and high concentrations of curculigoside induced glucose analogue uptake by approximately 2.0- and 2.1-fold (p < 0.01) when compared to the control. On the other hand,

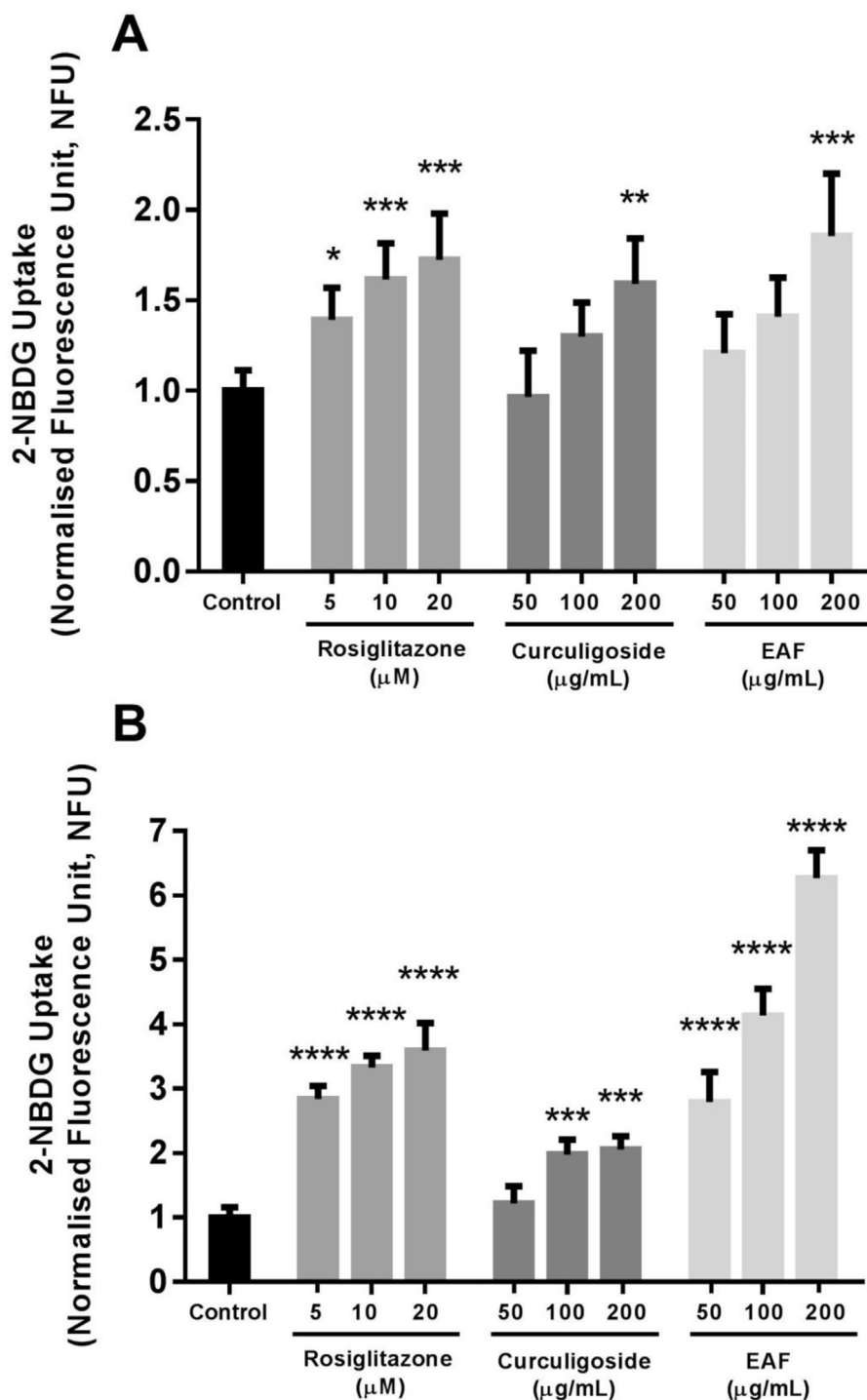


Fig. 2 – Effects of rosiglitazone, curculigoside and EAF on 2-NBDG uptake in differentiated 3T3-L1 adipocytes. (a) Under basal condition without insulin and (b) with the presence 100 nM insulin. Values are expressed as mean \pm standard deviation (n = 6). *p < 0.05, **p < 0.01, ***p < 0.001 and ****p < 0.0001 compared to the control.

2.8-, 4.1- and 6.3-fold ($p < 0.001$) increases in the uptake reaction were observed with the incubation with respective 50, 100 and 200 $\mu\text{g/mL}$ EAF.

Taken together, these results demonstrated the potential additive effect of curculigoside and EAF parallel to the action of insulin. Both curculigoside and EAF might act as insulin sensitizers that work by increasing the sensitivity of cells

towards the action of insulin. Interestingly, the efficacies of EAF in triggering uptake of glucose in the differentiated adipocytes were comparable to the use of rosiglitazone, an oral anti-diabetic agent from the thiazolidinedione class. In particular, 200 $\mu\text{g/mL}$ of EAF effectively enhanced the uptake of glucose by 120.3, 88.3 and 74.6% ($p < 0.05$) when compared to the respective treatments using 5, 10 and 20 μM rosiglitazone.

The administrations of anti-diabetic medications including biguanides and thiazolidinediones, as well as numerous medicinal plants and active phytoconstituents have manifested insulin-sensitising effects. However, the insulin-sensitising efficacies were also linked to increased adiposity and may further derange energy homeostasis [25,26]. In the present case, the use of curculigoside poses additional advantage for not inducing adipogenesis.

3.4. Unaltered PPAR γ expression

The process of adipocyte differentiation and uptake of glucose involve a series of programmed changes in the expression of certain genes and activation of the related proteins. In order to elucidate the underlying signalling cascades, the effect of curculigoside and EAF on the transcriptional expression of PPAR γ were investigated. As illustrated in Fig. 3, treatment with 200 $\mu\text{g}/\text{mL}$ of EAF up-regulated the mRNA expression of *Pparg* by 1.5-fold ($p < 0.05$) in comparison to control.

Contrarily, treatment with curculigoside did not render any differences in the transcriptional expression of *Pparg*. PPAR γ is the master regulator of adipocyte biology and has been associated with both *in vitro* and *in vivo* stimulation of adipogenesis [25]. The present results signified that the polyphenol-rich EAF might act by harnessing on the insulin sensitising effects of the nuclear receptor PPAR γ . While the activation of PPAR γ is generally linked to increased basal and insulin-stimulated glucose uptake, the potential weight gain may offset the beneficial effects [26]. Curculigoside, on the other hand, could potentially improve insulin sensitivity and hence, glucose uptake without promoting fat accumulation.

3.5. Curculigoside and EAF induce translocation of GLUT4 to the plasma membrane

The insulin-stimulated uptake of glucose into adipose tissues is regulated through trafficking of vesicles containing GLUT4 [27,28]. In this regard, the transcriptional and translational

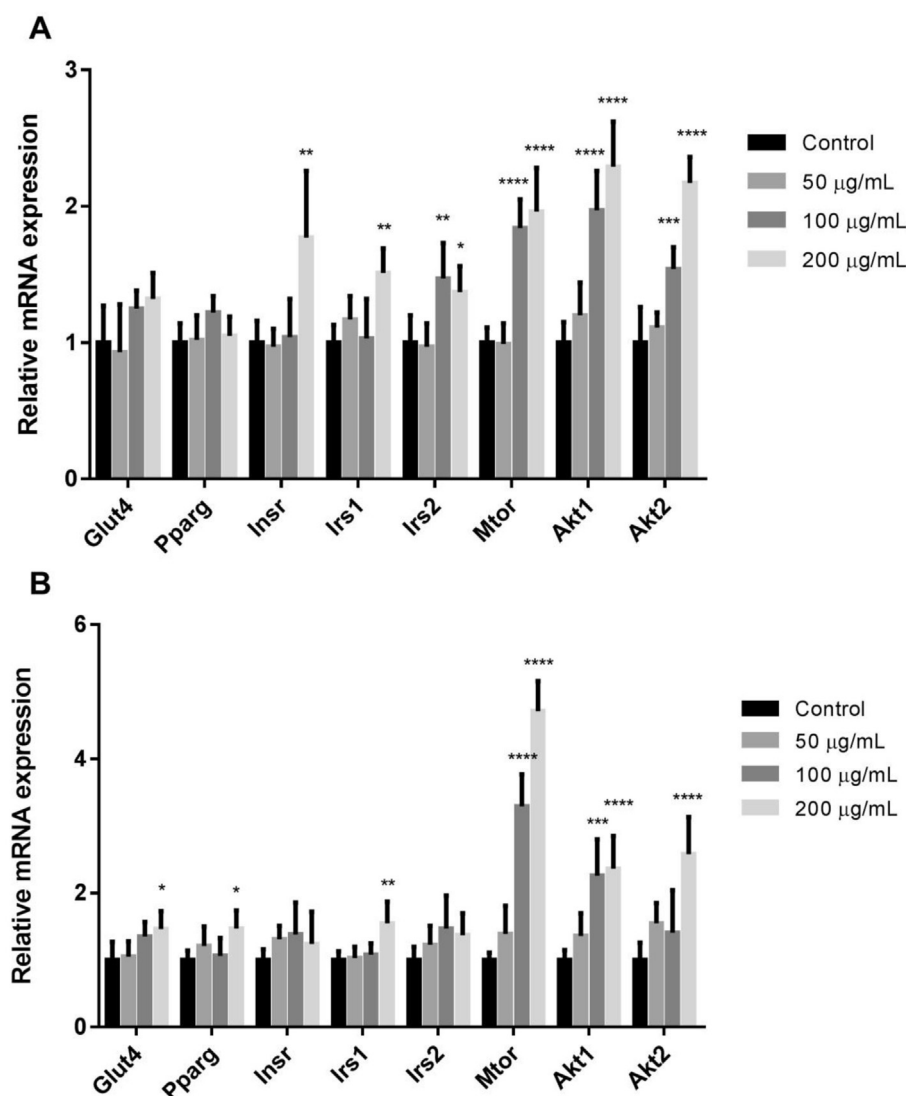


Fig. 3 – Relative mRNA expressions in differentiated 3T3-L1 adipocytes. Relative mRNA expressions in the presence of insulin and following treatments with (a) curculigoside and (b) EAF. Values are expressed as mean \pm standard deviation ($n = 6$). * $p < 0.05$, ** $p < 0.01$, *** $p < 0.001$ and **** $p < 0.0001$ compared to the control.

expressions of GLUT4 were subsequently studied (Figs. 3 and 4B). Curculigoside did not exert any effect on the regulation of *Glut4* expression, at both mRNA and protein levels. While EAF up-regulated the mRNA expression of *Glut4* by 1.5-fold ($p < 0.05$), the protein levels of GLUT4 were of no significant difference among the treatments. Following the observation, subcellular fractionation was performed to investigate the translocation of GLUT4 vesicles. Fig. 4C depicts increased availability of GLUT4 at the plasma membrane of treated adipocytes in comparison to IR- β . The redistribution of GLUT4 took place in a dose-dependent manner for both curculigoside and EAF. Both curculigoside and EAF did not trigger translocation of GLUT4 at the lowest concentration.

However, the medium and high concentrations of curculigoside respectively induced the translocation of GLUT4 by 1.8- and 2.1-fold ($p < 0.01$) when compared to the normal control. EAF stimulated a slightly higher response in which comparison to normal control revealed that its medium and high concentrations respectively elevated the GLUT4 expression at plasma membrane by 1.9- and 2.5-fold ($p < 0.01$).

Moreover, 200 $\mu\text{g/mL}$ of EAF also recorded a significant fold increase (1.5-fold; $p < 0.01$) when compared to the amount of GLUT4 translocation stimulated by insulin alone. The results suggested that the dynamic redistribution of GLUT4 at the plasma membrane might facilitate and bestow efficient transport of glucose observed in the present study.

3.6. Curculigoside and EAF regulate insulin signal transduction via activation of *Mtor* and *akt*

Transcriptional and translational expressions of selected intermediates in the insulin signalling pathway were further evaluated in pursuing the mechanism by which curculigoside and EAF exerted their effects. In general, both curculigoside and polyphenol-rich EAF affected the mRNA expressions of insulin receptor substrate 1 (*Irs1*), mechanistic target of rapamycin (*Mtor*), as well as v-akt murine thymoma viral oncogene homologue 1 and 2 (*Akt1* and *Akt2*), whereby the latter triggered greater fold changes in the aforementioned genes.

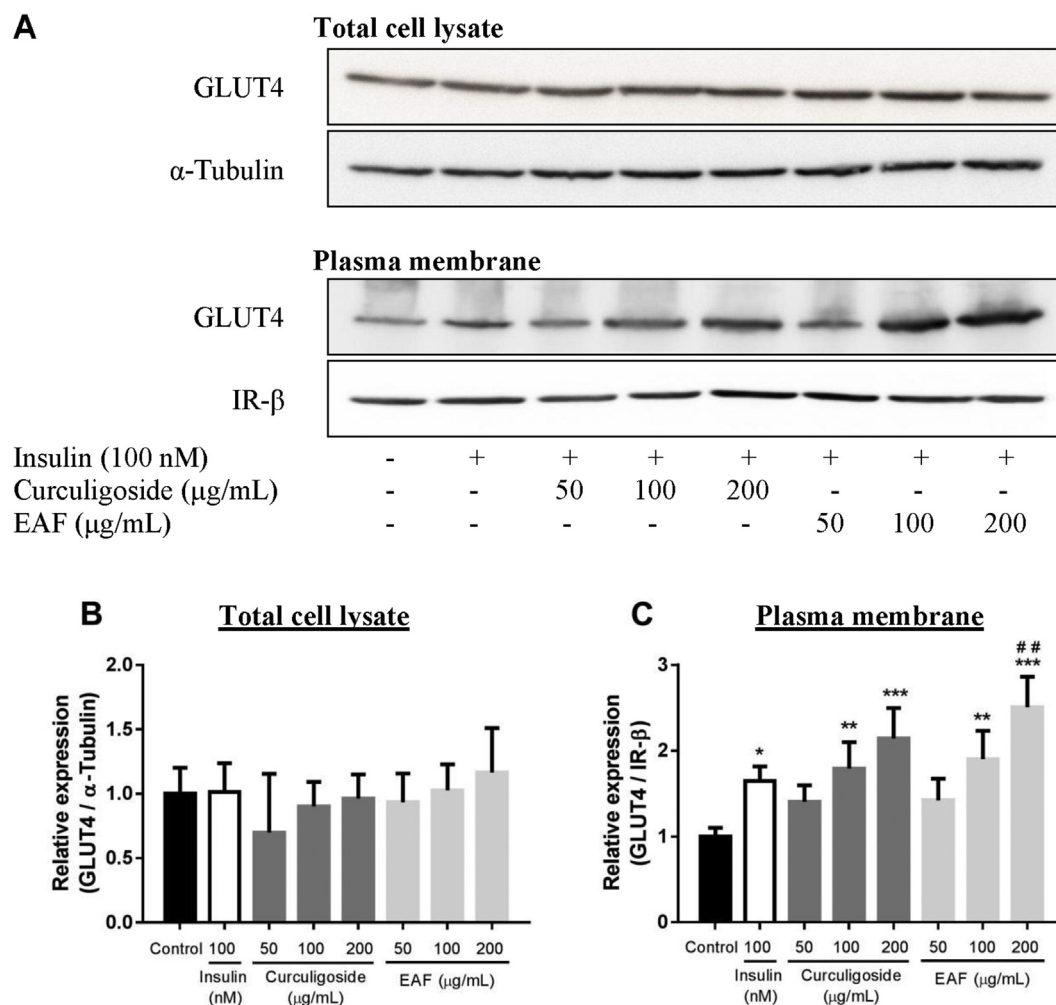


Fig. 4 – Effects of curculigoside and EAF on GLUT4 protein expression in differentiated 3T3-L1 adipocytes. (a) Representative immunoblot images. Relative protein expression of (b) GLUT4 in the total cell lysate and (c) GLUT4 in the plasma membrane of treated cells. α -Tubulin and IR- β were respectively being used as the loading control for total cell lysate and plasma membrane preparations. Values are expressed as mean \pm standard deviation ($n = 3$). * $p < 0.05$, ** $p < 0.01$ and *** $p < 0.001$ compared to the control; # $p < 0.05$ and ## $p < 0.01$ compared to the insulin control.

Comparison with normal control showed that the medium and high concentrations of curculigoside respectively increased the mRNA expressions of *Mtor* (1.8- and 2.0-fold; $p < 0.001$), *Akt1* (2.0- and 2.3-fold; $p < 0.001$) and *Akt2* (1.5- and 2.2-fold; $p < 0.01$). As for EAF, the medium and high concentrations respectively elevated the mRNA expressions of *Mtor* (3.3- and 4.7-fold; $p < 0.001$) and *Akt1* (2.3- and 2.4-fold; $p < 0.001$). The mRNA expression of *Akt2* was also up-regulated after the treatment with 200 $\mu\text{g}/\text{mL}$ EAF. In comparison to the normal control, there was 2.6-fold ($p < 0.001$) increase in the expression of *Akt2*.

Based on the results of transcriptional study, translational analyses of selected proteins were subsequently performed. The protein expression of AKT, p-AKT (Ser473), mTOR, p-mTOR (Ser2448) and α -tubulin from total cell lysate are shown in Fig. 5. Despite increased mRNA expression of *Akt1* and *Akt2*, the protein expression of total AKT did not significantly vary. Nevertheless, increased expressions of p-AKT (Ser473) in insulin-, curculigoside- and EAF-treated cells were noted. In comparison to the control, treatment with insulin increased AKT serine 473 phosphorylation by 1.3-fold ($p < 0.05$) while the highest concentration of curculigoside increased the expression of p-AKT (Ser473) by 1.9-fold ($p < 0.01$). Similarly, the p-AKT (Ser473) was also up-regulated in the treatment with 100 $\mu\text{g}/\text{mL}$ (1.7-fold; $p < 0.05$) and 200 $\mu\text{g}/\text{mL}$ (1.7-fold; $p < 0.05$) of EAF when compared to the control. Furthermore, 200 $\mu\text{g}/\text{mL}$ of both curculigoside and EAF also recorded a significant fold increase in AKT serine 473 phosphorylation (1.5- and 1.5-fold; $p < 0.01$ and $p < 0.01$) when compared to the insulin treatment alone.

On the other hand, the translational expression of mTOR was found to be significantly higher in the adipocytes incubated with 200 $\mu\text{g}/\text{mL}$ EAF. An approximate increase of 1.5-fold ($p < 0.05$) was observed when compared to the normal control. Comparison to the insulin treatment control also revealed significant fold increase (1.8-fold; $p < 0.01$). Interestingly, elevated amount of phosphorylated mTOR was also observed among the curculigoside- and EAF- treated adipocytes. The amount of p-mTOR (Ser2448) was up-regulated in the treatment with 100 $\mu\text{g}/\text{mL}$ (1.6-fold; $p < 0.01$) and 200 $\mu\text{g}/\text{mL}$ (1.6-fold; $p < 0.01$) of curculigoside. In comparison to the normal control, increased amounts of p-mTOR (Ser2448), ranging from 1.6- to 1.8-fold ($p < 0.01$ to $p < 0.001$), were observed with the various concentrations of EAF treatment. However, only the treatment with 200 $\mu\text{g}/\text{mL}$ of EAF demonstrated significant increase in phosphorylated mTOR (1.3-fold; $p < 0.05$) when compared to the insulin treatment control.

The mTOR pathway is involved in the regulation of many major cellular processes, as well as the onset and progression of disease states including cancer, diabetes, obesity, cardiovascular disease and neurodegeneration. Its regulation is affected by a wide range of cellular signals, including growth factors, energy levels, stress conditions, as well as oxygen and nutrients availability [29]. It is well known that mTOR interacts with different proteins in forming two biochemically and functionally distinct mTOR complexes, mTORC1 and mTORC2. While both mTORC1 and mTORC2 mediate different sensitivity towards rapamycin that acts as mTOR inhibitor, extensive crosstalk between the two complexes have been reported [30].

The activation of mTOR involves a complex series of upstream inputs and downstream outputs. In the insulin signalling cascades, activation of AKT results in direct or indirect phosphorylation of mTOR and exerts differential effects on the two mTOR complexes. In adipose tissue specifically, activation of mTORC1 leads to PPAR γ -mediated adipogenesis. Conversely, reduced lipolysis and increased uptake of glucose via GLUT4 translocation were observed with mTORC2-AKT activation [31–33]. Taken together, treatments with curculigoside and EAF were proposed to induce potential activation of mTORC2-AKT, subsequently promote the trafficking of GLUT4 at the plasma membrane and facilitate glucose uptake. In order to verify the potential target and molecular mode of action for both curculigoside and EAF, the use of specific pathway inhibitors including Akt inhibitors, PI3K inhibitors and mTOR inhibitors are further warranted.

3.7. Chemical composition of polyphenol-rich EAF and insulin sensitising effect

The polyphenol-rich EAF was previously analysed by HPLC-DAD analysis and non-targeted HPLC-QTOF mass spectrometry. The HPLC-DAD analysis showed that EAF comprised of 9.05% (w/w) of curculigoside, 1.24% (w/w) of cinnamic acid, 0.18% (w/w) of syringic acid and 0.03% (w/w) of ferulic acid [11]. On the other hand, non-biased phytochemical analysis of EAF by HPLC-QTOF mass spectrometry disclosed a total of 23 unique mass signals. Spectral database matching based on elemental composition data from accurate mass measurements of each peak putatively identified 18 compounds, of which most of them belong to the group of polyphenols [34,35].

The structural diversity of polyphenols in EAF has been proposed to effectively increase the bioactivity of the extract, potentially due to multi-targeted action, synergistic or complementary interactions present among all the compounds. In particular, hydroxycinnamic acid and its derivatives have been reported to demonstrate therapeutic benefit in experimental diabetes by regulating energy homeostasis, inflammation and insulin resistance [36]. 6-Gingerol, a pungent compound, has been demonstrated to regulate hepatic glucose metabolism and promote glucose uptake via GLUT4 translocation [37]. Isorhamnetin may act as PPAR γ antagonist, thus improving insulin resistance and hepatic steatosis [38]. Other than polyphenols, patented gibberellin-based formulations derived from terpenoid phytohormone gibberellic acid also suggest potential diabetes treatment efficacy (Patent reference US 20050215496 A1).

Although the flavanone hesperetin has been demonstrated to impair glucose uptake by suppressing proximal insulin signalling and inhibiting insulin-induced relocation of GLUT4 [39], the compound has also reported therapeutic potential for diabetes by inhibiting pro-inflammatory cytokine secretion, scavenging reactive oxygen species and modulating the PI3K/Akt and Wnt/ β -catenin signalling [40,41]. Interestingly, hesperetin and trans-resveratrol that were ineffective in individual experimental treatment, nevertheless, act synergistically to increase the expression of glyoxalase 1 enzyme, thereby increasing insulin sensitivity and conferring beneficial metabolic effects in overweight and obese populations [42].

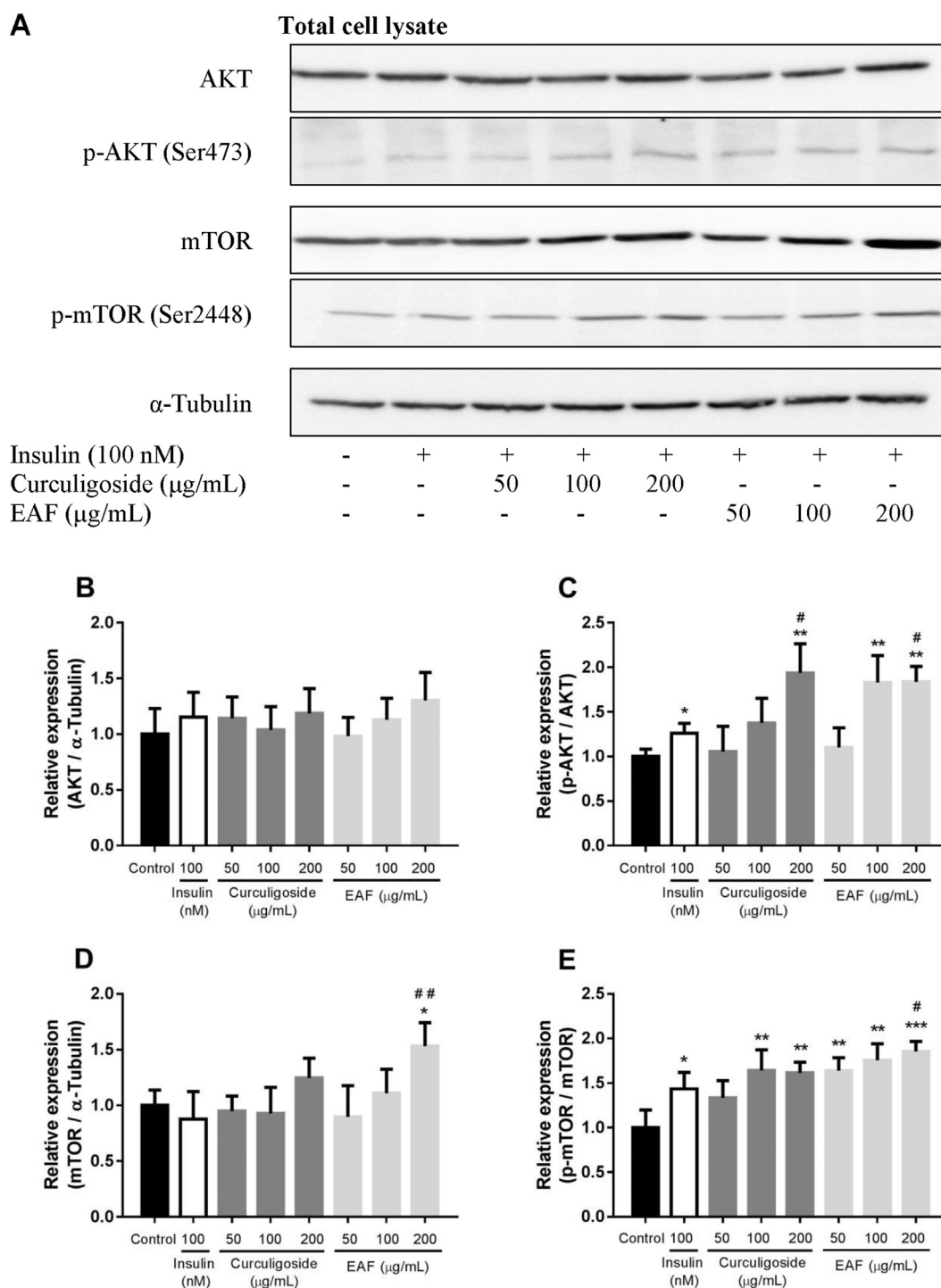


Fig. 5 – Effects of curculigoside and EAF on the protein expression of AKT, p-AKT, mTOR and p-mTOR in differentiated 3T3-L1 adipocytes. (a) Representative immunoblot images. Relative protein expression of (b) AKT, (c) p-AKT, (D) mTOR and (E) p-mTOR in the total cell lysate of treated cells. α -Tubulin was being employed as the loading control. Values are expressed as mean \pm standard deviation ($n = 3$). * $p < 0.05$, ** $p < 0.01$ and *** $p < 0.001$ compared to the control; # $p < 0.05$ and ## $p < 0.01$ compared to the insulin control.

Although the plethora amount of active constituents adds to the complexity of compound isolation and characterisation, deciphering the relationships between the chemical structure of each phenolic component in EAF and their insulin sensitising effect could intensify the

understanding on potential synergistic, additive or antagonistic effects of these constituents [43]. Thus, despite favourable outcome in the present study, a full characterisation on the preparations of EAF is needed and remains to be elucidated.

4. Conclusion

In summary, the present data suggested that curculigoside and EAF effectively improved uptake of glucose by increasing the availability of GLUT4 at the plasma membrane of differentiated 3T3-L1 adipocytes. These effects were at least partially mediated through potential activation of AKT and mTOR signalling cascades at the molecular level. In order to further substantiate the findings, research studies employing specific pathway inhibitors, as well as individual and compounding studies of the major and minor polyphenols are necessary and remain to be elucidated. The present results provided a fundamental basis for animal or human experimentation to further consolidate the therapeutic potentials of curculigoside and EAF for diabetes management.

Funding

This work was supported by Universiti Putra Malaysia via Research University Grant Scheme Initiative 2 (Project No. 04-02-12-2086RU) and Initiative 6 (Project No. 04-02-11-1381RU).

Conflicts of interest

The authors declare no conflicts of interest.

Acknowledgments

The authors gratefully acknowledge the assistance of staff members from the Laboratory of Molecular Biomedicine and Laboratory of Vaccine and Immunotherapeutics in completing the study.

Appendix A. Supplementary data

Supplementary data related to this article can be found at <https://doi.org/10.1016/j.jfda.2018.03.003>.

REFERENCES

- [1] Stöckli J, Fazakerley DJ, James DE. GLUT4 exocytosis. *J Cell Sci* 2011;124:4147–59.
- [2] Samuel VT, Shulman GI. Integrating mechanisms for insulin resistance: common threads and missing links. *Cell* 2012;148:852–71.
- [3] Soccio RE, Chen ER, Lazar MA. Thiazolidinediones and the promise of insulin sensitization in type 2 diabetes. *Cell Metabol* 2014;20:573–91.
- [4] Cariou B, Charbonnel B, Staels B. Thiazolidinediones and PPAR γ agonists: time for a reassessment. *Trends Endocrinol Metabol* 2012;23:205–15.
- [5] Consoli A, Formoso G. Do thiazolidinediones still have a role in treatment of type 2 diabetes mellitus? *Diabetes Obes Metabol* 2013;15:967–77.
- [6] Kang Z, Zhu H, Luan H, Han F, Jiang W. Curculigoside A induces angiogenesis through VCAM-1/Egr-3/CREB/VEGF signaling pathway. *Neuroscience* 2014;267:232–40.
- [7] Tian Z, Yu W, Liu H, Zhang N, Li X, Zhao M, et al. Neuroprotective effects of curculigoside against NMDA-induced neuronal excitotoxicity in vitro. *Food Chem Toxicol* 2012;50:4010–5.
- [8] Wang YK, Hong YJ, Wei M, Wu Y, Huang ZQ, Chen RZ, et al. Curculigoside attenuates human umbilical vein endothelial cell injury induced by H₂O₂. *J Ethnopharmacol* 2010;132:233–9.
- [9] Yin W, Qizhen S, Liyan M. Study on the effects of curculigoside on proliferation, differentiation, and calcification of mouse osteoblastic MC3T3-E1 cells. *World Sci Technol* 2011;13:852–5.
- [10] Peng J, Jiang Y, Fan G, Chen B, Zhang Q, Chai Y, et al. Optimization suitable conditions for preparative isolation and separation of curculigoside and curculigoside B from *Curculigo orchioides* by high-speed counter-current chromatography. *Separ Purif Technol* 2006;52:22–8.
- [11] Ooi DJ, Chan KW, Sarega N, Alitheen NB, Ithnin H, Ismail M. Bioprospecting curculigoside-cinnamic acid rich fraction from *Molineria latifolia* rhizome as potential antioxidant therapeutic agent. *Molecules* 2016;21:682.
- [12] Ishak NA, Ismail M, Hamid M, Ahmad Z, Abd Ghafar SA. Antidiabetic and hypolipidemic activities of curculigo latifolia fruit:root extract in high fat fed diet and low dose STZ induced diabetic rats. *Evid Based Compl Alternat Med* 2013;2013. e601838.
- [13] Imam MU, Ismail M, Ooi DJ, Azmi NH, Sarega N, Chan KW, et al. Are bioactive-rich fractions functionally richer? *Crit Rev Biotechnol* 2015;36:585–93.
- [14] The plant list. Version 1.1. 2013. Available online: <http://www.theplantlist.org>. [Accessed 13 April 2017].
- [15] Foo JB, Yazan LS, Tor YS, Armania N, Ismail M, Imam MU, et al. Induction of cell cycle arrest and apoptosis in caspase-3 deficient MCF-7 cells by *Dillenia suffruticosa* root extract via multiple signalling pathways. *BMC Compl Alternative Med* 2014;14:197.
- [16] Beh JE, Khoo LT, Latip J, Abdullah MP, Alitheen NBM, Adam Z, et al. SDF7, a group of *Scoparia dulcis* Linn. derived flavonoid compounds, stimulates glucose uptake and regulates adipocytokines in 3T3-F442a adipocytes. *J Ethnopharmacol* 2013;150:339–52.
- [17] Jung CH, Lee DH, Ahn J, Lee H, Choi WH, Jang YJ, et al. γ -Oryzanol enhances adipocyte differentiation and glucose uptake. *Nutrients* 2015;7:4851–61.
- [18] Nishiumi S, Ashida H. Rapid preparation of a plasma membrane fraction from adipocytes and muscle cells: application to detection of translocated glucose transporter 4 on the plasma membrane. *Biosci Biotechnol Biochem* 2007;71:2343–6.
- [19] Ali AT, Hochfeld WE, Myburgh R, Pepper MS. Adipocyte and adipogenesis. *Eur J Cell Biol* 2013;92:229–36.
- [20] Tung Y-C, Hsieh P-H, Pan M-H, Ho C-T. Cellular models for the evaluation of the antiobesity effect of selected phytochemicals from food and herbs. *J Food Drug Anal* 2017;25:100–10.
- [21] Wang W, Zhang Y, Lu W, Liu K. Mitochondrial reactive oxygen species regulate adipocyte differentiation of mesenchymal stem cells in hematopoietic stress induced by arabinosylcytosine. *PLoS One* 2015;10. e0120629.
- [22] Wang X, Hai C. Redox modulation of adipocyte differentiation: hypothesis of “Redox Chain” and novel insights into intervention of adipogenesis and obesity. *Free Radic Biol Med* 2015;89:99–125.
- [23] Bano G. Glucose homeostasis, obesity and diabetes. *Best Pract Res Clin Obstet Gynaecol* 2013;27:715–26.

- [24] Lowe CE, O'Rahilly S, Rochford JJ. Adipogenesis at a glance. *J Cell Sci* 2011;124:2681–6.
- [25] Lefterova MI, Haakonsson AK, Lazar MA, Mandrup S. PPAR γ and the global map of adipogenesis and beyond. *Trends Endocrinol Metabol* 2014;25:293–302.
- [26] Ahmadian M, Suh JM, Hah N, Liddle C, Atkins AR, Downes M, et al. PPAR γ signaling and metabolism: the good, the bad and the future. *Nat Med* 2013;19:557–66.
- [27] Leto D, Saltiel AR. Regulation of glucose transport by insulin: traffic control of GLUT4. *Nat Rev Mol Cell Biol* 2012;13:383–96.
- [28] Lizunov VA, Stenkula K, Troy A, Cushman SW, Zimmerberg J. Insulin regulates Glut4 confinement in plasma membrane clusters in adipose cells. *PLoS One* 2013;8:3.
- [29] Laplante M, Sabatini DM. mTOR signaling in growth control and disease. *Cell* 2012;149:274–93.
- [30] Foster KG, Fingar DC. Mammalian target of rapamycin (mTOR): conducting the cellular signaling symphony. *J Biol Chem* 2010;285:14071–7.
- [31] Pereira MJ, Palming J, Rizell M, Aureliano M, Carvalho E, Svensson MK, et al. mTOR inhibition with rapamycin causes impaired insulin signalling and glucose uptake in human subcutaneous and omental adipocytes. *Mol Cell Endocrinol* 2012;355:96–105.
- [32] Yoon M-S, Zhang C, Sun Y, Schoenherr CJ, Chen J. Mechanistic target of rapamycin controls homeostasis of adipogenesis. *J Lipid Res* 2013;54:2166–73.
- [33] Welch C, Zhen J, Bassène E, Raskin I, Simon JE, Wu Q. Bioactive polyphenols in kinkéliba tea (*Combretum micranthum*) and their glucose-lowering activities. *J Food Drug Anal* 2018;26:487–96.
- [34] Ooi DJ, Chan KW, Ismail N, Imam MU, Ismail M. Polyphenol-rich ethyl acetate fraction of *Molineria latifolia* rhizome restores oxidant-antioxidant balance by possible engagement of KEAP1-NRF2 and PKC/NF- κ B signalling pathways. *J Funct Foods* 2018;42:111–21.
- [35] Ooi DJ, Adamu HA, Imam MU, Ithnin H, Ismail M. Polyphenol-rich ethyl acetate fraction isolated from *Molineria latifolia* ameliorates insulin resistance in experimental diabetic rats via IRS1/AKT activation. *Biomed Pharmacother* 2018;98:125–33.
- [36] Alam MA, Subhan N, Hossain H, Hossain M, Reza HM, Rahman MM, et al. Hydroxycinnamic acid derivatives: a potential class of natural compounds for the management of lipid metabolism and obesity. *Nutr Metab* 2016;13:27.
- [37] Son MJ, Miura Y, Yagasaki K. Mechanisms for antidiabetic effect of gingerol in cultured cells and obese diabetic model mice. *Cytotech* 2015;67:641–52.
- [38] Zhang Y, Gu M, Cai W, Yu L, Feng L, Zhang L, et al. Dietary component isorhamnetin is a PPAR γ antagonist and ameliorates metabolic disorders induced by diet or leptin deficiency. *Sci Rep* 2016;6:19288.
- [39] Yang Y, Wolfram J, Boom K, Fang X, Shen H, Ferrari M. Hesperetin impairs glucose uptake and inhibits proliferation of breast cancer cells. *Cell Biochem Funct* 2013;31:374–9.
- [40] Lee A, Yun J-M. Hesperetin inhibits pro-inflammatory cytokine secretion induced by lipopolysaccharide in differentiated human THP-1 monocytes under hyperglycemic conditions. *FASEB J* 2017;31:1b339.
- [41] Kim SY, Lee J-Y, Park Y-D, Kang KL, Lee J-C, Heo JS. Hesperetin alleviates the inhibitory effects of high glucose on the osteoblastic differentiation of periodontal ligament stem cells. *PLoS One* 2013;8. e67504.
- [42] Xue M, Weickert MO, Qureshi S, Kandala N-B, Anwar A, Waldron M, et al. Improved glycemic control and vascular function in overweight and obese subjects by glyoxalase 1 inducer formulation. *Diabetes* 2016;65:2282–94.
- [43] Herranz-López M, Fernández-Arroyo S, Pérez-Sánchez A, Barrajón-Catalán E, Beltrán-Debón R, Menéndez JA, et al. Synergism of plant-derived polyphenols in adipogenesis: perspectives and implications. *Phytomedicine* 2012;19:253–61.